

# Characterization of Dielectric Properties of Graphene and Graphite Using the Resonant Cavity in 5G Test Band

Vinicius M. Pereira<sup>1</sup> , Luis G. Hardt<sup>1</sup> , Dieison G. Fantineli<sup>2</sup> , Marcos V. T. Heckler<sup>3</sup> ,  
Luis E. G. Armas<sup>1</sup> 

<sup>1</sup>Grupo de Óptica, Micro e Nanofabricação de Dispositivos - GOMNDI, Universidade Federal do Pampa - UNIPAMPA, CEP 97546-550, Campus Alegrete, Rio Grande do Sul, Brazil

[viniciusmp2.aluno@unipampa.edu.br](mailto:viniciusmp2.aluno@unipampa.edu.br), [luisvieira.aluno@unipampa.edu.br](mailto:luisvieira.aluno@unipampa.edu.br), [luisarmas@unipampa.edu.br](mailto:luisarmas@unipampa.edu.br),  
<sup>2</sup>Laboratório de Metalografia e Tratamentos Térmicos, Universidade Federal do Pampa – UNIPAMPA, CEP 97546-550, Campus Alegrete, Rio Grande do Sul, Brazil [dieisonfantineli@unipampa.edu.br](mailto:dieisonfantineli@unipampa.edu.br)

<sup>3</sup>Laboratório de Electromagnetismo, Micro-Ondas e Antenas, Universidade Federal do Pampa-UNIPAMPA, CEP 97546-550, Campus Alegrete, Rio Grande do Sul, Brazil  
[marcosheckler@unipampa.edu.br](mailto:marcosheckler@unipampa.edu.br)

**Abstract**— This paper presents a study about the dielectric constant  $\epsilon_r$ , dielectric loss tangent  $\tan g(\delta)$  and effective electrical conductivity  $\sigma_e$  of graphene, graphite and graphene-bakelite combination using the resonant cavity method. For this purpose, cylindrical samples with diameter of 30 mm and thickness of 4.5 mm were analyzed taking into account the central frequency  $f_0 = 3.5$  GHz, according to 5G technology standards. The constants  $\epsilon_r$  and  $\tan g(\delta)$  were obtained from the resonance frequency  $f_a$  of measured scattering parameters (S-parameters), when the cavity was loaded with the samples. An empirical equation was developed to model the relation between  $f_a$  and  $\epsilon_r$ . With this empirical equation it was found  $\epsilon_r = 9.3203$  and  $\tan g(\delta) = 0.7000$  for graphene and  $\epsilon_r = 17.1508$  and  $\tan g(\delta) = 0.2700$  for graphite. The addition of bakelite in combination with graphene allowed controlling the dielectric properties of these composites. The results, obtained in this macroscale characterization, are interesting for Telecommunications Engineering, especially in the development of radiation-absorbent material, which is suitable for mitigation of interference between different wireless communication systems.

**Index Terms**— Dielectric constant, dielectric loss constant, resonant cavity, graphene, graphite.

## I. INTRODUCTION

The investigation of dielectric properties of materials is particularly interesting for Telecommunications Engineering, especially in Microwave Engineering, Antenna Theory and industry of devices for communication systems. Among these properties, the relative electrical permittivity ( $\epsilon_r$ ) and the dielectric loss tangent ( $\tan g(\delta)$ ) can be considered the most relevant ones [1], [2]. In the last years, graphene has become the most interesting carbon allotrope for the development of new materials, because of its promising possibilities in terms of technological

applications [3]. In this context, the investigation of the dielectric properties of graphene and graphite is relevant, since it supports new potential applications.

In terms of molecular arrangement, graphene is formed by long two-dimensional chains whose unit cells have hexagonal geometry, derived from connections of carbon atoms, ideally of the  $sp^2$ -type. A specific configuration case of this system is the micro-structural configuration of graphite, in which the two-dimensional chains are superimpose forming a three-dimensional structure [2]-[4].

Considering microscale analysis, graphene exhibits excellent electrical conduction capability. For this reason, graphene films (with thicknesses of the order of nanometers) can be used as electrically conductive structures in the design of nano-antennas for communications in the higher bands (higher than 10 GHz) of the 5<sup>th</sup> generation of mobile communication systems (5G). Sa'don et al. presented a study about the design of a single element and an array of graphene printed antennas, in coplanar-waveguide (CPW) technology for operation frequency at 15 GHz [5]. This structure consists in a graphene layer with thickness of 100 nm, printed on a Kapton film substrate with thickness of 76  $\mu\text{m}$ . The authors reported gain values of 2.87 dBi and 9.28 dBi for the single element and the array antennas, respectively.

On the other hand, taking into account macroscale analysis, graphene can be also used as “inserted component” in radiation-absorbent material (RAM). Tantis et al. showed the insertion of two-dimensional graphene structures into polymeric matrices - poly(vinyl alcohol) nanocomposites [6]. Four different concentrations of graphene oxide were considered (1-3 wt% and 5 wt%). The authors observed that the variation of graphene oxide inserted into the matrix controls its dielectric constant and dielectric loss tangent values. Bispo et al. described a study about the different polymeric composites production based on polystyrene matrix [7]. The composites produced with xerogel, carbon-graphene and graphite presented the most efficient results in terms of electromagnetic absorption in X-band (8.2 - 12.4 GHz), where about 87% of the incident electromagnetic power was absorbed by these samples. These analyses were performed considering the macroscale effects of graphene interacting with electromagnetic fields.

The use of resonant cavities is a classic approach for the determination of the properties  $\epsilon_r$  and  $\tan \delta$  of dielectric materials. This device is typically hollow, with metallic walls composing a cylindrical or a rectangular shape. When a dielectric sample with  $\epsilon_r > 1$  is inserted into the cavity, its resonance frequency  $f_0$  decreases, due to perturbation of the internal electromagnetic field. From this frequency shift, the  $\epsilon_r$  constant of the sample can be derived [8]-[10]. The reports by Rubinger and Costa [11] and Zhang et al. [12] used the resonant cavity method for characterization of dielectric constants of polymeric samples. These parameters were mathematically obtained with specific equations, proposed by the authors, so as to link the measured frequency (for each sample) to the  $\epsilon_r$  constant. In general, up to now, there are several studies about the dielectric properties

characterization of graphene and graphite at different frequencies [13]-[15], but not at 3.5 GHz using the resonant cavity method.

Therefore, taking into account the previous comments, in this work, an experimental study for the macroscale characterization of dielectric and loss tangent constants of graphite, graphene and graphene-bakelite combinations using a cylindrical resonant cavity is presented. Initially, the technical details of the design and fabrication of the cavity are presented. Then, a mathematical modeling of this experimental setup is derived and empirical equations for  $\epsilon_r$  and  $\tan g(\delta)$  assessments are proposed. This approach is validated by the characterization of samples in macroscale, whereby graphene and graphite demonstrated to have large loss constants in the 5G test frequency 3.5 GHz. This feature indicates that both are potential candidates to be used in the development and production of new radiation-absorbent materials (RAMs). This property is very interesting to mitigate inference between different wireless communication systems.

The next section presents the methodology used in this study. In section 3, the procedure for preparation of the samples and the used materials are described. The measured data (in terms of resonance frequency for each sample) and estimations for  $\epsilon_r$ ,  $\tan g(\delta)$  and  $\sigma$  are presented and discussed in section 4. Finally, the conclusions of this work are drawn.

## II. DESIGN OF THE EXPERIMENTAL SETUP

### A. Design of the resonant cavity

The design frequency ( $f_0$ ) was defined as 3.5 GHz, because this is the testing frequency for the development of new technologies for the 5G systems [16] [17]. Next, the cavity geometry has been defined to be cylindrical, due to fabrication issues. The cavity dimensions have been optimized using the electromagnetic simulator ANSYS HFSS<sup>®</sup> software and are summarized in Table I, where  $a$  is the inner radius,  $d$  is the inner height and  $l$  is the length of the excitation elements (copper wires).

TABLE I. PHYSICAL DIMENSIONS OF THE CYLINDRICAL RESONANT CAVITY

Dimension	Optimized Value (mm)
$a$	32.40
$d$	41.50
$l$	7.56

The prototype of this resonant cavity was divided in two parts: the hollow main body and the cover. The excitation elements have been attached to the latter. Both parts were produced with aluminum, with the dimensions  $a$  and  $d$  as listed in Table I, and are shown in Fig. 1 (a) and (b). The excitation elements, which consist of two female SMA connectors with inner conductors extended with copper wires coated with nylon polymer, are shown in Fig. 1 (c).

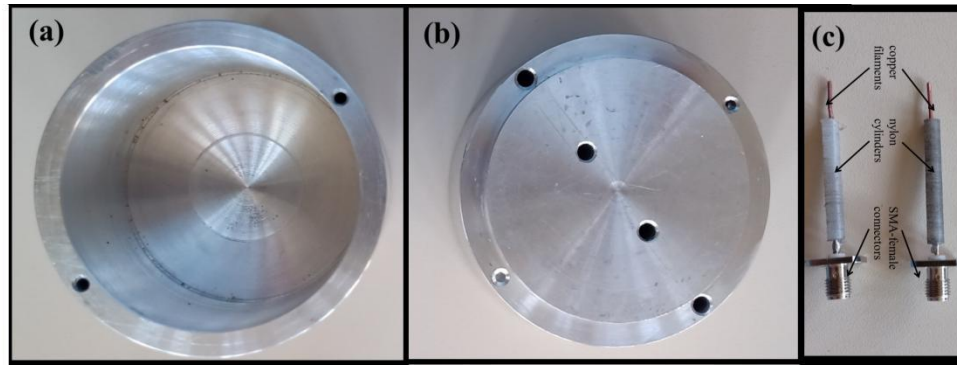


Fig. 1. Parts of the cylindrical resonant cavity prototype: (a) Hollow main body; (b) Cover and (c) Excitation elements.

A vector network analyzer (VNA) model E5071C (Agilent Technologies) was used for the measurements of the  $S$ -parameters for the resonant cavity loaded with graphene, graphite and graphene-bakelite samples. The resonance frequency of the loaded cavity  $f_a$  can be obtained with this setup and is determined by assessing the frequency for which the lowest value of  $S_{11}$  is verified. The dielectric constants, of each sample can be estimated from  $f_a$  with an empirical mathematical equation formulated for  $\epsilon_r$ , whereas the loss tangent can be assessed by parametric simulations with ANSYS HFSS<sup>®</sup>. The  $\tan g(\delta)$  parameter is varied in the simulation model, and its experimental value can be inferred since that, the simulated value of  $S_{21}$  approaches the magnitude of the measured  $S_{21}$  in the pass-band.

#### B. Mathematical Modeling for the $\epsilon_r$ and $\tan g(\delta)$ calculation

The dielectric constant of the samples is calculated from  $f_a$ , obtained from the measured  $S_{11}$  - parameter, when the sample is placed inside the resonant cavity. For the  $\epsilon_r$  calculation, a parametric study was performed in ANSYS HFSS<sup>®</sup> software, by varying  $\epsilon_r$  from 2 to 20, with a step of 1, in order to assess the resulting  $f_a$  values and to allow estimating the most appropriate equation for the modeling of the proposed experimental setup.

The mathematical representation is based on the literature for the generalized equations for modeling the perturbation in the resonant cavity [18] and experimental studies presented by Rubinger and Costa [11] and Costa et al. [19]. In these papers, the authors show that  $\epsilon_r$  is related to  $(f_0 - f_a)/f_0$  ratio through an empirical equation, which holds exclusively for a given setup (in terms of geometry and dimensions of the cavity and of the samples). The general representation of this relation is given by [18].

$$(f_0 - f_a)/f_0 = F(\epsilon_r - 1) \quad (1)$$

From the most suitable function  $F(x)$  (with  $x = \epsilon_r - 1$ ) that describes the relation between  $\epsilon_r$  and  $f_a$ , the argument  $x$  can be isolated and estimated according to the measured  $f_a$  for each characterized

sample. Finally, considering  $\varepsilon_r = x + 1$ , the dielectric constant for each sample can be calculated.

From the generalized representation given by Eq. (1), the mathematical modeling of the present study is developed. In the present study, the samples exhibit cylindrical shape with diameter of 30 mm and thickness of 4.5 mm. The obtained data in parametric analysis with ANSYS HFSS® simulator are listed in Table II. In Fig. 2, the graphical representation of this “calibration curve” for  $(f_0 - f_a) / f_0$  as a function of  $\varepsilon_r - 1$  is presented.

The mathematical representation that adequately describes the calibration curve in Fig. 2 is given by:

$$(f_0 - f_a) / f_0 = 0.0108 \ln(\varepsilon_r - 1) + 0.0158 \quad (2)$$

Isolating the term  $\varepsilon_r$ , the final form of the mathematical representation for this experimental setup is given by

$$\varepsilon_r = e^{\left[ \frac{(f_0 - f_a) / f_0 - 0.0158}{0.0108} \right]} + 1 \quad (3)$$

TABLE II. VALUES OF  $f_a$  (GHz) OBTAINED WITH THE PARAMETRIC ANALYSES WITH ANSYS HFSS®

$\varepsilon_r$	$\varepsilon_r - 1$	$f_a$ (GHz)	$(f_0 - f_a) / f_0$
2	1	3.4350	0.0157
3	2	3.4070	0.0238
4	3	3.3930	0.0278
5	4	3.3820	0.0309
6	5	3.3740	0.0332
7	6	3.3670	0.0352
8	7	3.3600	0.0372
9	8	3.3560	0.0384
10	9	3.3520	0.0395
11	10	3.3510	0.0398
12	11	3.3450	0.0415
13	12	3.3410	0.0427
14	13	3.3400	0.0430
15	14	3.3350	0.0444
16	15	3.3330	0.0450
17	16	3.3300	0.0458
18	17	3.3260	0.0470
19	18	3.3250	0.0473
20	19	3.3190	0.0490

These equations are valid only for the mathematical modeling for the proposed setup and for the 5G test frequency 3.5 GHz. For other cases, e.g. other frequency of interest, a new calibration curve must be obtained using the methodology explained here.

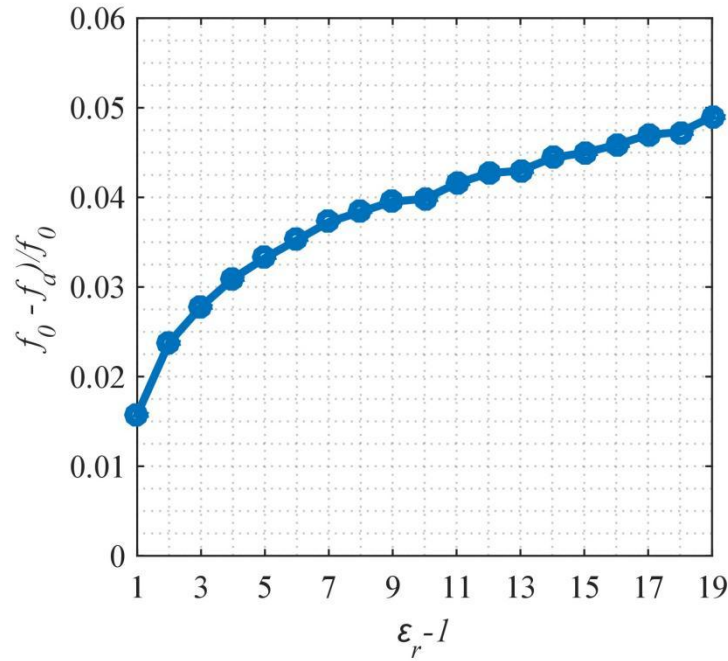


Fig. 2. Calibration curve for the experimental setup designed in this work.

### C. Calculation of Effective Electrical Conductivity

The general mathematical representation of  $\tan g(\delta)$  relates to electrical conductivity as

$$\tan g(\delta) = \frac{\sigma_0 + \omega \epsilon''}{\omega \epsilon'} \quad (4)$$

Where,  $\sigma_0$  denotes the static electrical conductivity (S/m),  $\omega = 2\pi f_a$  is the angular frequency, in rad/s,  $\epsilon'$  and  $\epsilon''$  are the real and imaginary components of the electrical permittivity, given in F/m [20].

The term  $\omega \epsilon''$  can be also identified as the component of effective electrical conductivity ( $\sigma_e$ ) due to the imaginary part of the electrical permittivity. Thereby,

$$\sigma_e = \omega \epsilon''$$

$$\sigma_e = \sigma_0 + \sigma_\alpha \quad (5)$$

Finally, replacing (5) in (4), we can obtain

$$\tan g(\delta) = \frac{\sigma_e}{\omega \epsilon'} \quad (6)$$

With this equation, one can estimate the effective electrical conductivity from the calculated  $\tan g(\delta)$  for each sample [20].

### D. Samples Specifications

The commercial graphene and graphite used in this work were provided by the Brazilian companies Amazonas Grafeno and Nacional Grafite, respectively. Fig. 3 shows an image MEV (a), where it is possible to see the graphene layers, and an average Raman spectrum ( $\sim 14$  spectra taken at different places of one sample) (b) with its characteristic Raman bands (D, G, 2D e 2D'), of the graphene

powder used to prepare the samples. For these measurements the powder was placed on a SiO<sub>2</sub> substrate using the micromechanical method. In order to verify the number of graphene layers the integrated intensity ratio  $I_{2D}/I_G$  was calculated, finding the value of  $\sim 0.6$ . It is well known that, for free-defect graphene, the  $I_{2D}/I_G$  is dependent on the number of graphene layers [21]. The ratio  $I_{2D}/I_G \sim 2-3.5$  is for monolayer graphene,  $1 < I_{2D}/I_G < 2$  for bilayer graphene and  $I_{2D}/I_G < 1$  for few layers graphene (FL) as shown on Fig. 3(a). The samples were produced using the embedding process.

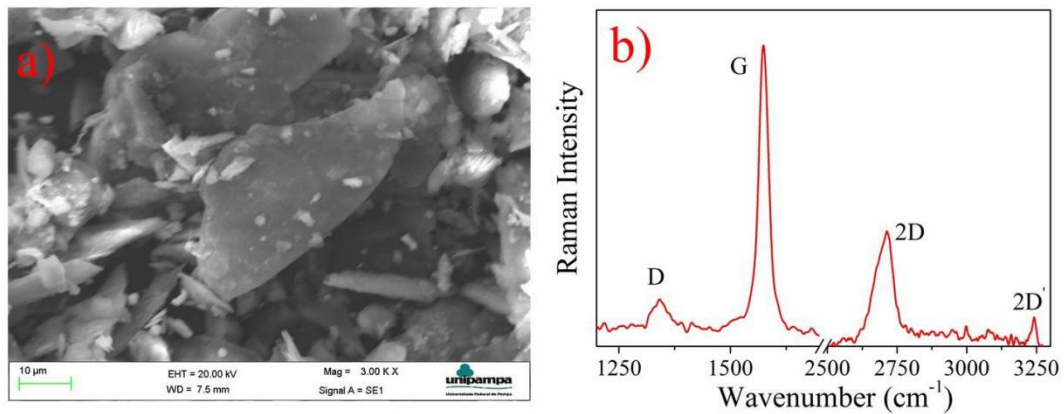


Fig. 3. (a) Image MEV and (b) average Raman spectrum of few layers of commercial graphene (Amazonas).

Fig. 4 shows samples of graphene (gn100) (a) and graphite (gt100) (b) produced from powdered materials (5.5251 g for graphene, and 5.8939 g for graphite), which were singly entered in a hydraulic piston at a constant pressure of 1000 lb/inch<sup>2</sup> and by applying a heating ramp from 25 °C to 145 °C during 7 minutes. The top temperature (145 °C) was then kept during additional 8 minutes. The final result is a pastille formed by the aggregation of powdered particles.

The zoomed pictures of the samples gn100 and gt100 (shown in Fig. 4(a) and (b)) are homogeneous and uniform, with some clusters of the material (white dots), indicating that the embedding process was effective in compacting the powder materials.

Samples based on the mixture of three different combinations of graphene and bakelite (powdered polymer that becomes solid) with the procedure described above were also produced for the verification of dielectric properties. The concentration (in %) of graphene and bakelite and their respective masses (g) are shown in Table III.

TABLE III. COMPOSITION OF THE BAKELITE-GRAPHENE SAMPLES

Proportion: Bakelite-graphene	bakelite (g)	graphene (g)
100% - 0% (bk100)	5.5534	0.0000
60% - 40% (gn40)	3.3322	2.3490
50% - 50% (gn50)	2.7767	2.9398
40% - 60% (gn60)	2.2214	3.5262

The resulting bakelite-graphene samples are shown in Figs. 4 (c) – (e). The addition of bakelite in these mixtures results in the hardest samples to handle and are more suitable for experimental characterization. As seen for the samples gn100 and gt100 (Fig. 4 (a) and (b)), the zoomed pictures of the samples gn40, gn50 and gn60 (shown Fig. 4 (c - e)), taken with a x10 objective lens of an optical microscope, are also homogeneous and uniform to investigate the dielectric properties at the frequency of 3.5 GHz. It is worth to emphasize that, this frequency can be still considered as low frequency, and then the sample surface does not show significant irregularities that compromise the results at this frequency.

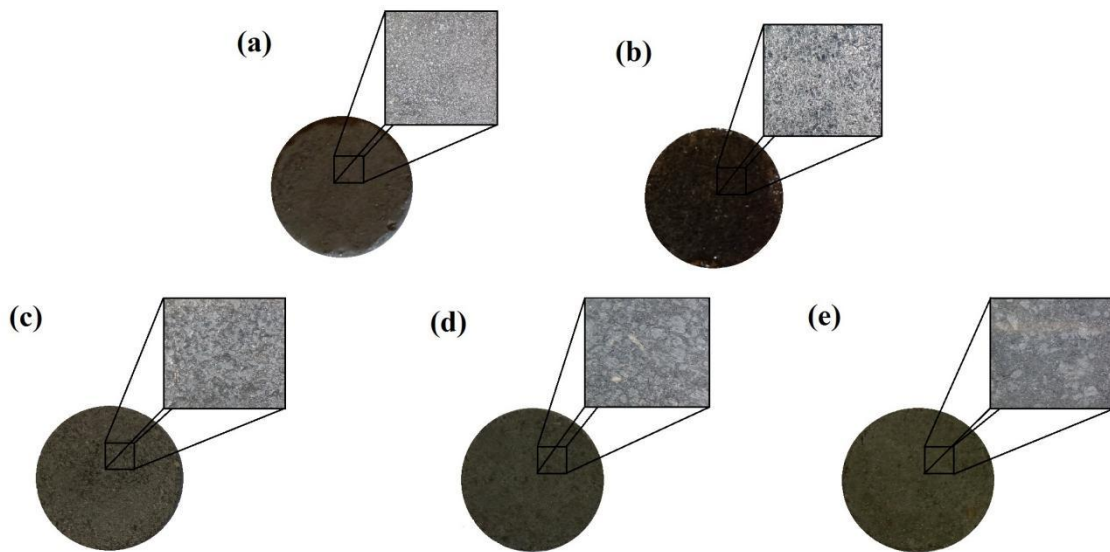


Fig. 4. Produced graphene and graphite samples: (a) gn100 and (b) gt100 and Bakelite-graphene produced samples (c) gn40; (d) gn50 and (e) gn60.

### III. EXPERIMENTAL RESULTS

The samples described in the previous section were inserted, one at a time, into the resonant cavity and the  $S$ -parameters were measured. Fig. 5 shows a comparison of the  $S_{11}$  (a) and  $S_{21}$  (b) parameters for gn100 and gt100 samples with the measured parameters considering the unloaded cavity (UC, blue curves of  $S_{11}$  and  $S_{21}$ ). In both cases, the minimum values of  $S_{11}$  and maximum of  $S_{21}$ . The results obtained are plotted in Fig. 5 for samples gn100 and gt100. These measured values for the graphite sample exhibit larger shifts to lower frequencies when compared to the graphene sample. This behavior indicates that the dielectric constant of graphite is higher than that of graphene. According to Fig. 5 (a), the resonance frequency of the cavity loaded with the sample gn100 is  $f_a = 3.3550$  GHz and, for gt100, it is  $f_a = 3.3300$  GHz. Using these values, the estimated dielectric constants are  $\epsilon_r = 9.3203$  for graphene and  $\epsilon_r = 17.1508$  for graphite.

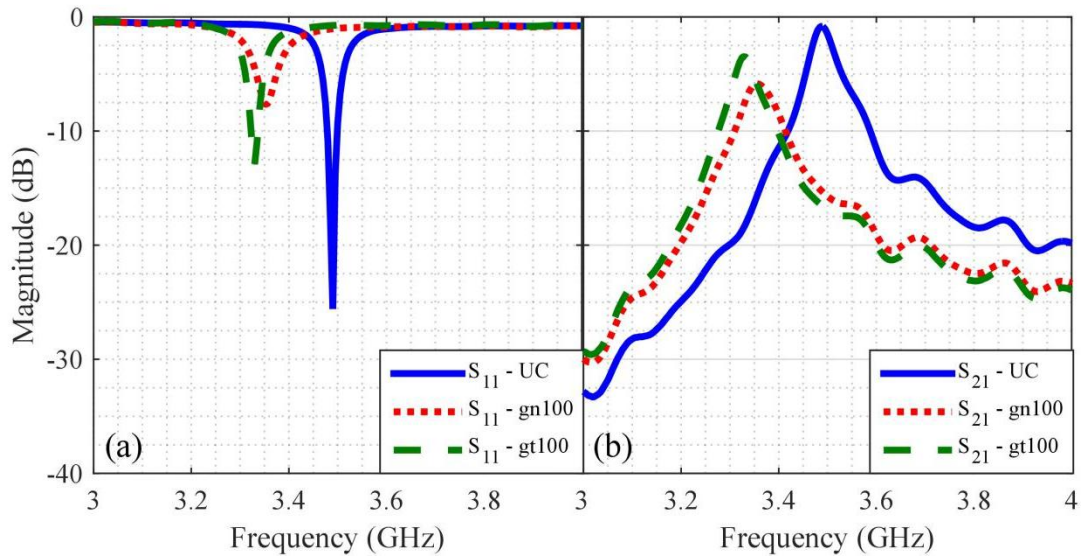


Fig. 5. Measured (a)  $S_{11}$ -parameters and (b)  $S_{21}$  parameters for samples gn100 and gt100.

As mentioned before, most studies about the dielectric properties characterization of graphene, reported in the literature, consider the analysis of nanometric structures and its results are very divergent from each other. In a different way, the present work considers the dielectric properties characterization of graphene in macroscale. For instance, Bessler et al. [22] characterized the resulting dielectric constant of a bilayer graphene (BLG) with the atomic force microscopy (AFM) technique. Their analyzed the effects of the microscopic structure of the material and the interactions between the two graphene layers, reporting a dielectric constant of  $\epsilon_r = 6.0000$ , for BLG. However, Cismaru et al. [23] obtained a different experimental result using a different characterization method. In their study, a single layer graphene (SLG) was deposited on a gold substrate to compose a coplanar waveguide (CPW) structure. Their samples were characterized from 5 to 40 GHz, obtaining  $\epsilon_r \approx 16.00$  at the frequency of 5 GHz. The difference between our results with those reported by other authors is attributed to the use of different characterization techniques applied at different frequencies. The cited studies developed graphene characterization in microscale, while this work considers the characterization of graphene in macroscale and at a lower frequency than the reported by the authors. According to this, we can argue that different characterization methods and frequencies of analysis will give different responses of the dielectric properties.

For instance, Hotta et al. [24] has presented the characterization of dielectric properties of carbonaceous materials, considering frequencies from 1 GHz to 10 GHz, using the rectangular section waveguide method. In this study, the measured  $\epsilon_r$  constant for the graphite sample is equal to 17.00 in the frequency of 3.5 GHz. Additionally, the authors report that the  $\epsilon_r$  constant of graphite change as the frequency characterization changes. Therefore, we can infer that the characterization methodology adopted in this work is able to provide reliable estimation for  $\epsilon_r$ .

As shown in Fig 5 (b), the peak magnitude of the measured  $S_{21}$ -parameter in  $f_a = 3.3550$  GHz for the gn100 sample is -5.8510 dB. For gt100 sample, it is -3.4430 dB at  $f_a = 3.3300$  GHz. The peak magnitude of the measured  $S_{21}$ -parameter for the unloaded cavity is -0.8210 dB. This reduction in the peak magnitude for the loaded cavity demonstrates the influence of the  $\tan g(\delta)$  constant on the analyzed materials. For the determination of dielectric loss tangents of the samples, some parametric simulations in ANSYS HFSS® software, considering the calculated  $\epsilon_r$  constant for each sample, were performed. The correct value of  $\tan g(\delta)$  is the one where the simulated  $S_{21}$ -parameter curve approaches the corresponding measured  $S_{21}$ -parameter curve.

According to this procedure, the gn100 sample has  $\tan g(\delta) = 0.7000$  and the gt100 sample has  $\tan g(\delta) = 0.2700$ . These dielectric loss tangent values are very high and the characterized materials can be considered as very good electromagnetic absorbers at the frequency of interest. These materials have the capability to dissipate energy in its structure, hence producing large attenuation of the electromagnetic waves. For instance, for the gn100 sample, 68.45% of the power coupled to the cavity is dissipated by the sample, and, for gt100, this reduces to 45.32%. Hotta et al. [24] verified that  $\tan g(\delta) \approx 0.5294$  for graphite. This difference can be explained because the authors did not directly characterized this property, but estimated with theoretical equations.

Fig. 6 (a) and (b) show the  $S_{11}$  and  $S_{21}$ -parameters for samples manufactured by bakelite-graphene combinations. Measured  $S_{11}$ -parameters for the loaded cavity with 40% graphene and 50% graphene samples (gn40 and gn50) resulted in  $f_a$  values very close to each other, resulting in  $\epsilon_r$  values slightly different, as shown in Table IV. However, the sample gn60 (with 60% graphene) presented the same result obtained with sample gn100, i.e.  $f_a = 3.3550$  GHz and  $\epsilon_r = 9.3203$ . Table 4 shows the  $\epsilon_r$  constants calculated for these analyzed samples along with the obtained  $\tan g(\delta)$  constant in the parametric simulations in ANSYS HFSS® software.

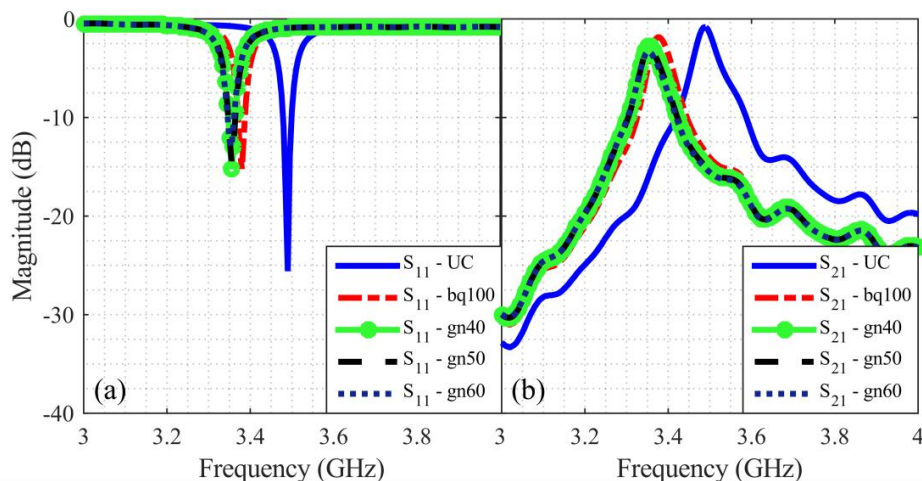


Fig. 6. Measured (a)  $S_{11}$ -parameters and (b)  $S_{21}$ -parameters for bakelite-graphene combinations samples.

According to the results presented in Fig. 6 (a) and (b) and the numerical results listed in Table IV, different bakelite-graphene combinations yield different electromagnetic absorption capacity in comparison to the experimental response for sample gn100 (see Fig. 7 (a) and (b)). The dielectric-loss constant of bakelite (sample bk100) is lower than that one of graphene. The characterization of the reference sample resulted in  $f_a = 3.3750$  GHz,  $\epsilon_r = 5.8940$  and  $\tan g(\delta) = 0.0840$ . Therefore, the combination of two materials with different characteristics results in a composite with properties that can be controlled based on their concentrations: higher graphene concentrations result in composites with higher  $\tan g(\delta)$  and  $\epsilon_r$  values, whereas higher bakelite concentrations result in composites with lower  $\tan g(\delta)$  and  $\epsilon_r$  constants.

TABLE IV. DIELECTRIC PROPERTIES OF THE BAKELITE-GRAPHENE CHARACTERIZED SAMPLES

sample	$f_a$ (GHz)	$\epsilon_r$	Measured		$\tan g(\delta)$
			$S_{21f}$ (dB)	Simulated $S_{21f}$ (dB)	
UC	-	-	-0.8210	-0.1101	-
bk-100	3.3750	5.8940	-1.8390	-1.1280	0.0840
gn40	3.3585	8.5825	-2.7010	-1.9902	0.1410
gn50	3.3565	8.9957	-2.9800	-2.2692	0.1720
gn60	3.3550	9.3203	-3.3330	-2.6223	0.2480

These experimental data demonstrate the linear relation (region between dashed red lines) existing between  $\epsilon_r$  and the bakelite concentration (in %). The variation of  $\epsilon_r$  and  $\tan g(\delta)$  is inversely proportional to the bakelite concentration, as shown in Fig. 7(a) and (b). Therefore, the parameters  $\epsilon_r$  and  $\tan g(\delta)$  on the graphene composites tend to decrease accordingly as the concentration of a material with lower constants  $\epsilon_r$  and  $\tan g(\delta)$  increases.

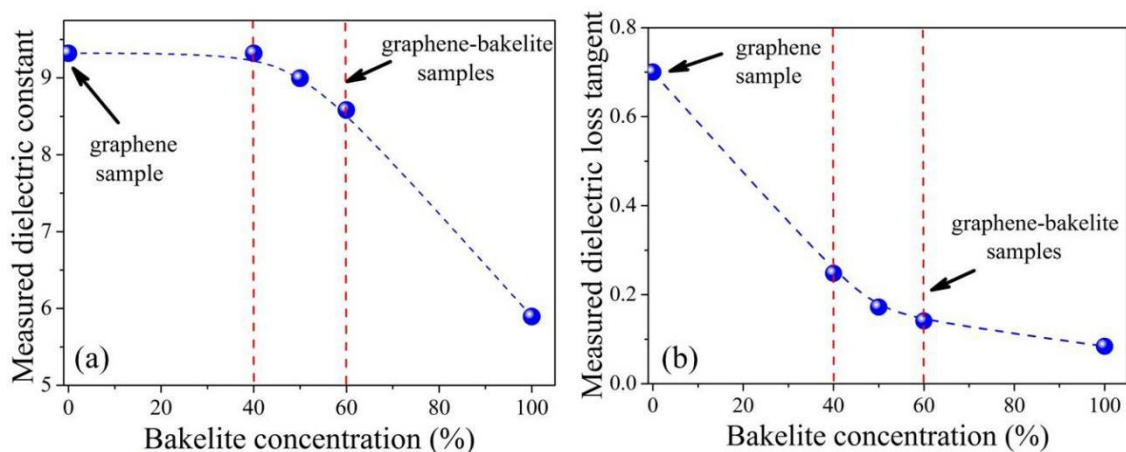


Fig. 7. Effect of different bakelite concentration on (a) dielectric constant and (b) dielectric loss tangent.

The effect of increasing  $\epsilon_r$  constant with the addition of higher concentrations of graphene in the samples was also reported by others authors, considering different frequencies of analysis and matrix materials, but their results indicates the same department related in the present work. For instance,

Bispo et al. [7] produced and characterized the dielectric properties of samples based in a polymeric matrix (polystyrene) with insertion of 10% of Carbon-Graphene Xerogel (CGX). The resulting measured dielectric constant (considering X-band, 8.2 – 12.4 GHz) was  $\epsilon_r$  (CGX) = 4.00. However, the reference sample (100% polystyrene) had a dielectric constant  $\epsilon_r$  (matrix) = 2.99. And, Liu et al. [23] also verified that the insertion of different concentrations of graphene oxide in a polyimide matrix resulted in different  $\epsilon_r$  constants. For the highest concentration of graphene oxide (1%) the measured dielectric constant was 8.00 and the dielectric constant of the reference sample (100% polyimide resin) was  $\epsilon_r$  (matrix) = 3.50. These experimental results were obtained at 1 MHz.

The increase of  $\tan g(\delta)$  for higher concentrations of graphene in the samples was also observed by Liu et al. [25] even though considering different conditions of frequencies of analysis and matrix material. The authors verified that the insertion of different concentrations of graphene oxide in a polyimide resin matrix resulted in samples with different dielectric-loss constants. For the highest concentration of graphene oxide (1%) the measured  $\tan g(\delta)$  was 0.12 with  $\tan g(\delta)$  (matrix) = 0.02 for the reference sample (100% polyimide resin). These experimental parameters were also obtained at 1 MHz.

According to these experimental results, it is convenient to state that the insertion of controlled concentrations of graphene into a specified matrix causes the increase of their dielectric properties  $\epsilon_r$  and  $\tan g(\delta)$ . It is worth also to emphasize that different authors have determined the dielectric properties of graphene oxide mixing them with different materials and at different frequencies, but as mentioned in the introduction section so far there are not studies of these properties on graphene in the 5G test band (3.5 GHz). These results can contribute for making use these dielectric properties for the development of new RAMs.

Finally, in Table V the estimated values of electrical conductivity, obtained with Eq. (6), for samples gt100, gn100, gn60, gn50 and gn40, are presented. The high values of  $\sigma_e$ , obtained for the samples gt100 ( $\sigma_e = 856.7000$  S/mm) and gn100 ( $\sigma_e = 1216.0000$  S/mm) reinforce the optimal quality of effective electrical conductivity of graphene and graphite.

Mohan et al. [26] reported the experimental characterization of the electrical conductivity of graphene oxide. The authors obtained the maximum value of  $\sigma_e = 100.0000$  S/mm for analyzed samples. On other hand, Marinho et al. [27] described that the electrical conductivity of compact graphene structures present values varying to the pressure applied in the samples. For minimal values of pressure (approximate to 0 MPa), the authors verified that  $\sigma_e \approx 100.0000$  S/mm for graphene sample.

Marinho et al. [27] also reported that the  $\sigma_e$  constant of compact graphite structures present values varying to the pressure applied in the samples. In this analysis, the authors showed that, for minimal

values of pressure applied in the compression of the samples, the resultant estimated electrical conductivity of sample based in graphite with density equal to  $0.8600 \text{ g/cm}^3$  is  $\sigma_e \approx 900.0000 \text{ S/mm}$ . This specific result is comparable to the obtained in the present work for gt100 sample.

In addition, the mixture of bakelite with graphene causes a great reduction in  $\sigma_e$ . This fact can be explained because bakelite has  $\tan g(\delta)$  lower than graphene and, consequently, its electrical conductivity is also smaller. Then, its combination with graphene yields a composite with reduced electrical conducting capacity.

TABLE V. CALCULATED VALUES OF ELECTRICAL CONDUCTIVITY OF SAMPLES FROM GRAPHITE, GRAPHENE AND GRAPHENE-BAKELITE COMBINATIONS

sample	$\tan g(\delta)$	$\sigma_e$ (S/mm)
gt100	0.2700	856.7000
gn100	0.7000	1216.0000
gn60	0.1410	430.8000
gn50	0.1720	288.5000
gn40	0.2480	225.8000

## V. CONCLUSION

In this work, we reported the characterization of dielectric properties of graphene, graphite and different combinations of bakelite-graphene, considering the test band of 5G (3.5 GHz), and compared these obtained data with previous works found in the literature. Samples entirely produced from graphene and graphite, and samples produced from three different combinations of graphene and bakelite, were analyzed. The high experimental values obtained suggest that these carbonaceous materials are very interesting for the development of technologies for electromagnetic radiation absorbing materials in the radiofrequency spectrum. It was demonstrated in the analysis of bakelite-graphene samples that it is possible to control the dielectric properties of the composites according to the adequate choice of the proportional concentrations of graphene and the matrix material (bakelite, in this work) in the same way as described in the literature. This is very interesting for different applications such as Stealth devices and absorbers materials for anechoic chambers. In addition, the optimal characteristic of electrical conductivity for graphene and graphite also was verified by means of the estimates for  $\sigma_e$  constant from the  $\tan g(\delta)$  data. These values are in agreement with other studies previously reported in the literature.

## ACKNOWLEDGMENTS

The authors would like to thank to Coordenação de Aperfeiçoamento de Pessoal de Nível Superior - CAPES for the fellowship to V. M. Pereira; to CNPq for the fellowship to Luis E. G. Armas; and the Federal University of Pampa – UNIPAMPA for Experimental facilities.

REFERENCES

- [1] P. Bretchko, RF Circuit Design: Theory and Applications. Prentice-Hall, 2000.
- [2] T. S. Mailadil, *Dielectric Materials for Wireless Communication*, 2008.
- [3] D. Verma, K. LimGoh, Functionalized Graphene Nanocomposites and their Derivatives Synthesis, *Processing and Applications, Micro and Nano Technologies*, pp.219-243, 2019.
- [4] C. Jin, H. Lan, L. Peng, K. Suenaga and S. Lijima, Deriving Carbon Atomic Chains from Graphene, *Phys. Rev. Lett.*, 102, pp. 205501, 2009.
- [5] S. N. H. Sa'don, M. H. Jamaluddin, M. R. Kamarudin, F. Ahmad, Y. Yamada, K. Kamardin and I. H. Idris. "Analysis of Graphene Antenna Properties for 5G Applications", *Sensors*, vol. 19, pp. 4835-4854, 2019.
- [6] L. Tantis, G. Psarras, and D. Tasis, "Functionalized Graphene-poly (vinil alcohol) Nanocomposites: Physical and Dielectric Properties", *Express Polymer Letters*, vol. 6 no. 4, 2012.
- [7] M. C. Bispo, B. H. K. Lopes, B. C. D. S. Fonseca, R. C. Portes, J. T. Matsushima, M. K. H. Yassuda, G. Amaral-Labat, M. R. Baldan, and A. C. D. C. Migliano, "Electromagnetic Properties of Carbon-Graphene Xerogel, Graphite and Ni-Zn Ferrite composites in Polystyrene Matrix in the X-band (8.2-12.4 GHz)", *Matéria (Rio de Janeiro)*, vol. 26, 2021.
- [8] Z. Li and E. Li, "Study on Measurement of Dielectric Constant of Partially Filled Material Using Modified Cavity Perturbation Technique", in *2012 International Workshop on Microwave and Millimeter Wave Circuits and System Technology*, pp. 1-3, 2012.
- [9] B. Liu, D. R. Slocombe, J. Wang, A. Aldawsari, S. Gonzalez-Cortes, J. Arden, V. L. Kuznetsov, H. AlMegren, M. AlKinany, T. Xiao, *et al.*, "Microwaves Effectively Examine the Extent and Type of Coking over Acid Zeolite Catalysts", *Nature Communications*, vol. 8, no. 1, pp. 1-7, 2017.
- [10] K. Li, J. Chen, J. Peng, R. Ruan, and C. Srinivasakannan, "Microwave Dielectric Properties and Thermochemical Characteristics of the Mixtures of Walnut Shell and Manganese Ore", *Bioresource Technology*, vol. 286, pp. 121381, 2019.
- [11] C. P. L. Rubinger and L. C. Costa, "Building a Resonant Cavity for the Measurement of Microwave Dielectric Permittivity of High Loss Materials", *Microwave and Optical Technology Letters*, vol. 49, no. 7, pp. 1687-1690, 2007.
- [12] H. Zhang, B. Q. Zeng, L. Ao, and Z. Zhang, "A Novel Dual-loop Coupler for One-port Cylindrical Cavity Permittivity Measurement", *Progress In Electromagnetics Research*, vol. 127, pp.537-552, 2012.
- [13] R. G. Geyer. "Dielectric Characterization and Reference Materials". NIST Technical Note 1338. National Institute of Standards and Technology, Department of Commerce. United States, 1990. <https://www.govinfo.gov/content/pkg/GOVPUB-C13319af9ee141c44f1f5c7072208f56b6b/pdf/GOVPUB-C13319af9ee141c44f1f5c7072208f56b6b.pdf>
- [14] R. Bessler, U. Duerig, and E. Koren, "The Dielectric Constant of a Bilayer Graphene Interface", *Nanoscale Advances*, vol. 1, no. 5, pp. 1702-1706, 2019.
- [15] A. Cismaru, M. Dragoman, A. Dinescu, D. Dragoman, G. Stavrinidis, and G. Konstantinidis, "Microwave and Millimeterwave Electrical Permittivity of Graphene Monolayer", arXiv Preprint arxiv:1309.0990, 2013.
- [16] ANATEL, Agência Nacional de Telecomunicações, "Frequências Destinadas ao 5G têm Novo Ato e Consulta sobre Requisitos Técnicos", 2020. In <https://www.anatel.gov.br/institucional/mais-noticias/2610-frequencias-destinadas-ao-5g-tem-novo-ato-e-consulta-sobre-requisitos-tecnicos>.
- [17] European Telecommunications Standards Institute, "Technologies", 2020. In <https://www.etsi.org/technologies/mobile/5g>.
- [18] D. M. Pozar, *Microwave Engineering*, 4<sup>th</sup> ed., 2011
- [19] L. C. Costa, A. Aoujgal, M. P. F. Graça, N. Hadik, M. E. Achour, A. Tachafine, J. C. Carru, A. Oueriagli, and A. Outzourit, "Microwave Dielectric Properties of the System Ba1-xSrxTiO3", *Physica B: Condensed Matter*, vol. 405, no. 17, pp. 3741-3744, 2010.
- [20] R. G. Geyer. "Dielectric Characterization and Reference Materials". NIST Technical Note 1338. National Institute of Standards and Technology, Department of Commerce. United States, 1990. <https://www.govinfo.gov/content/pkg/GOVPUB-C13319af9ee141c44f1f5c7072208f56b6b/pdf/GOVPUB-C13319af9ee141c44f1f5c7072208f56b6b.pdf>.
- [21] Lisiane S. Severo, Juliana B.Rodrigues, Dionathan A.Campanelli, Vinicius M.Pereira, Jacson W. Menezes, Eliana W. de Menezes, Chiara Valsecchi, Marcos A. Z.Vasconcellos and Luis E. G. Armas, Synthesis and Raman characterization of wood sawdust ash, and wood sawdust ash-derived graphene, *Diamond and Related Materials*, vol. 117, 108496 (2021).
- [22] R. Bessler, U. Duerig, and E. Koren, "The Dielectric Constant of a Bilayer Graphene Interface", *Nanoscale Advances*, vol. 1, no. 5, pp. 1702-1706, 2019.
- [23] A. Cismaru, M. Dragoman, A. Dinescu, D. Dragoman, G. Stavrinidis, and G. Konstantinidis, "Microwave and Millimeterwave Electrical Permittivity of Graphene Monolayer", arXiv Preprint arxiv:1309.0990, 2013.
- [24] M. Hotta, M. Hayashi, M. T. Lanagan, D. K. Agrawal, and K. Nagata, "Complex Permittivity of Graphite, Carbon Black and Coal Powders in the Ranges of X-band Frequencies (8.2 to 12.4 GHz) and between 1 and 10 GHz", *ISIJ International*, vol. 51, no. 11, pp. 1766-1772, 2011.
- [25] P. Liu, Z. Yao, and J. Zhou, "Mechanical, Thermal and Dielectric Properties of Graphene Oxide/Polyimide Resin Composite", *High Performance Polymers*, vol. 28, no. 9, pp. 1033-1042, 2016.
- [26] V. B. Mohan, R. Brown, K. Jayaraman and D. Bhattacharyya, "Characterization of Reduced Graphene Oxide: Effects of Reduction variables on Electrical Conductivity", *Materials Science and Engineering B*, vol 193, pp. 49-60, 2014.
- [27] B. Marinho, M. Ghislandi, E. Tkalya, C. E. Koning and G. de With, "Electrical Conductivity of Compacts of Graphene, Multi-wall Carbon Nanotubes, Carbon Black, and Graphite Powder", *Powder Technology*, vol. 221, pp. 351-358, 2012.